Carbohydrate Polymers **22** (1993) 161–173

Thermogelation of methylcellulose. Part I: molecular structures and processes

Anwarul Haque & Edwin R. Morris*

Department of Food Research & Technology, Cranfield University, Silsoe College, Silsoe, Bedford, UK, MK45 4DT

(Received 26 June 1993; accepted 12 July 1993)

Thermogelation of methylcellulose (A4M from Dow) shows two distinct 'waves' of increase in G', preceded by an initial reduction at lower temperature. The reduction and first wave of increase are accompanied by a sigmoidal change in optical rotation (indicating a co-operative conformational transition). Light transmission and detectable ^{1}H-NMR reach their maximum values at the end of the first structuring process, but drop to almost zero over the temperature range of the second. Both structuring processes are reversible on cooling, but offset to lower temperature, and are accompanied by enthalpy changes in DSC (endothermic on heating; exothermic on cooling). About 40% of the high-resolution NMR signal remains undetectable in the solution state at low temperature, and the shear rate dependence of viscosity is appreciably different from that of disordered polysaccharide coils.

The proposed interpretation of these findings is that methylcellulose chains exist in solution as aggregated 'bundles', held together by packing of unsubstituted or sparingly substituted regions of cellulosic structure, and by hydrophobic clustering of methyl groups in regions of denser substitution. As the temperature is raised, the ends of the bundles come apart, exposing methyl groups to the aqueous environment and causing a large increase in volume (with consequent increase in G'). At higher temperature the methyl substituents shed structured water, and form a hydrophobically crosslinked network (giving the second 'wave' of increase in G'). As in other polysaccharide systems, the thermal hysteresis is attributed to aggregation stabilising the cellulosic 'bundles' to temperatures higher than those at which they will re-form on cooling.

INTRODUCTION

Methyl and hydroxypropylmethyl derivatives of cellulose have the unusual property of forming gels on heating and reverting to the solution state on cooling, with many practical applications in industry (see, for example, Greminger & Savage, 1973; Grover, 1986). However, in contrast to the extensive literature on gelation of naturally occurring polysaccharides, there have been very few scientific publications on the molecular origin of the gelation behaviour of these hydrophobically substituted materials.

The first systematic investigation was by Heymann (1935), who used measurements of solution viscosity to monitor the onset of gel formation, and in particular to explore the lyotropic effects of different salts. More recently, Sarkar (1979) published an extensive study of the Methocel range of methylcellulose and hydroxypropylmethylcellulose (HPMC) products marketed by the Dow Chemical Company, and this remains the definitive experimental work on thermogelation of cellulose derivatives. Gel strength was characterised by compression testing, development of turbidity was followed by measurements of light transmission, and the temperature course of rheological change in the early stages of gelation was again monitored by measurement of solution viscosity.

At a more theoretical level, it is generally agreed that the driving-force to gelation or precipitation of hydrophobic polymers at elevated temperature is their disruptive effect on the structure of water (Rees, 1969; Tanford, 1980; Franks, 1983). As in any chemical process, the relative stabilities of the solution and gel states are determined by the difference in free energy

*To whom correspondence should be addressed.

Carbohydrate Polymers 0144-8617/93/$06.00

(ΔG) between them (Cantor & Schimmel, 1980), which is in turn determined by the (absolute) temperature (T) and the differences in enthalpy and entropy (ΔH and ΔS, respectively):

$$\Delta G = \Delta H - T\Delta S \quad (1)$$

Conversion from one state to the other will occur only when ΔG is negative (i.e. if the overall free energy of the system is decreased), which requires a negative value of ΔH and/or a positive value of ΔS. In thermal melting of normal polysaccharide gels, ΔS is positive, because of the increase in chain mobility, but ΔH is also positive, because the system must absorb heat to disrupt the bonding within the intermolecular 'junction zones' (Rees *et al.*, 1982). The two effects balance exactly at the transition-midpoint temperature (T_m), where $\Delta G = 0$:

$$\Delta H = T_m\Delta S \quad (2)$$

At higher temperatures $T\Delta S > \Delta H$, giving $\Delta G < 0$, so that the system shifts to the solution state. At lower temperature $T\Delta S < \Delta H$ and $\Delta G > 0$, favouring the gel state.

As a starting point for explaining why hydrophobically substituted polysaccharides should gel on heating rather than on cooling, it is useful to consider first the behaviour of simple hydrocarbons. Although their free energy is far higher in water than in most non-aqueous solvents, the enthalpy is lower (i.e. hydrocarbon–water interactions are more favourable than hydrocarbon–hydrocarbon interactions, so that in this sense 'hydrophobic' is a misnomer). The increase in free energy must therefore come from a decrease in entropy, which is normally interpreted (Tanford, 1980; Franks, 1983) as distortion of the hydrogen bonding between water molecules to give highly constrained 'cage-like' structures around the foreign species (if these cannot themselves form hydrogen bonds with water). One piece of direct evidence in favour of this interpretation is that when aqueous solutions of hydrocarbons (or other non-polar species, notably inert gases) are cooled, they may produce solid clathrates in which the guest species are indeed trapped within a hydrogen-bonded cage of water molecules.

Extrapolating this concept to apolar ('hydrophobic') substituents on polymers, the solution is now the low-entropy, low-enthalpy state (the exact reverse of the situation in conventional polysaccharide gels). Raising the temperature increases the relative importance of the entropy term, and therefore promotes gelation. It should be noted, however, that although both ΔH and ΔS have opposite sign in 'hydrophobic' and 'hydrophilic' gelation, their direction of change with temperature is the same in both cases: entropy increases on heating, and the enthalpy of the system also increases. Indeed we could (simplistically) regard hydrophobic gelation as a 'melting' process (disruption of the water 'cages'). Endothermic transitions on heating, and exotherms on cooling, are therefore to be expected for either hydrophobic interactions or enthalpically stabilised 'junction zones'.

Although the concept of hydrophobic substituents shedding their sheath of structured water and clustering together at high temperature goes a long way towards rationalising the phenomenon of thermogelation, it does not fully explain the behaviour of methylcelluloses. In particular, eqn (2) would predict that formation and dissociation of hydrophobic 'clusters' should have the same value of $T_m(\Delta H/\Delta S)$, but there is very substantial thermal hysteresis between the gelation and liquefaction temperatures of commercial Methocels (Sarkar, 1979).

Our own studies, reported here and in the following paper (Haque *et al.*, 1993*b*), arose from a (successful) attempt to produce acceptable bread from rice flour (which is devoid of gluten); a preliminary account has been published elsewhere (Haque *et al.*, 1993*a*). The innovative feature of the research was the use of dispersions of ispaghula husk to stabilise the gas-cell structure during proving (fermentation with yeast). To maintain stability at oven temperature, however, we followed the well established route of incorporating a small amount of HPMC (Greminger & Savage, 1973; Grover, 1986). The material used was Methocel K4M from Dow which, from practical experience, the manufacturers recommend as the most suitable grade for bread-making.

Preliminary studies of the temperature course of thermogelation of K4M showed an unexpected complexity of behaviour (Haque *et al.*, 1993*a*) which prompted us to carry out a fuller investigation. To avoid the additional complication of having two different chemical substituents present, we first explored the gelation and liquefaction of methylcellulose (A4M) from the same supplier. The results are reported here. The following paper (Haque *et al.*, 1993*b*) uses the understanding developed in the present work as a starting point for explaining the behaviour of HPMC.

INVESTIGATIVE TECHNIQUES

Temperature dependent changes in macromolecular organisation and functional interactions were characterised by a combination of spectroscopic and rheological methods that have proved informative in previous investigations of other polysaccharides.

Optical rotation

Optical rotation is well established as a sensitive probe of changes in the relative orientation of adjacent residues within carbohydrate chains (Rees *et al.*, 1982). The first application to gelling polysaccharides was in

studies of carrageenans, where sharp, sigmoidal changes were observed over the temperature range of the sol–gel transition, corresponding to conversion from disordered coils to the ordered double-helix structure that cross-links chains within the gel network. Similar sigmoidal changes in optical rotation have subsequently been reported as a correlate of order–disorder transitions in many other polysaccharide systems.

Differential scanning calorimetry

The formation and dissociation of ordered structures are normally accompanied by enthalpy changes that can be detected by sensitive calorimetric measurements (Wright, 1984). Where the molecular changes are induced by changes in temperature (as in thermoreversible gels) the appropriate technique is differential scanning calorimetry (DSC). Unlike optical rotation, DSC can be applied to turbid samples.

Signal intensity in high-resolution NMR

Disordered polysaccharide coils give NMR peaks only slightly broader than those in spectra of small molecules in solution. On conversion to rigid, ordered structures, however, the associated change in spin–spin relaxation time (T_2) causes extreme line-broadening, so that the high-resolution spectrum is flattened out into the baseline and becomes undetectable. The loss of detectable high-resolution NMR intensity can therefore be used as an additional probe of conformational ordering (Rees *et al.*, 1982). The technique can again be applied to turbid samples.

Transmission of light

Development of turbidity can be quantified by reduction in the amount of light transmitted through the sample. In the absence of significant changes in absorption, loss of transmission can be attributed to scattering by structures with dimensions comparable to the wavelength of light.

Solution viscosity

Solutions of disordered polysaccharide coils interacting only by physical entanglement show a characteristic, general form of 'shear thinning'. At low rates of deformation (shear rate, $\dot{\gamma}$), where forced disentanglement is balanced by formation of new entanglements between different chain partners, the viscosity (η) remains constant at the maximum 'zero-shear' value, η_0. At higher values of $\dot{\gamma}$, however, where the rate at which existing entanglements are pulled apart exceeds the rate at which new entanglements can form (Graessley, 1974), the viscosity decreases. The rate dependence of this behaviour can be conveniently characterised by $\dot{\gamma}_{1/2}$, the shear-rate at which η is reduced to half the maximum value (i.e. $\eta = \eta_0/2$ at $\dot{\gamma} = \dot{\gamma}_{1/2}$). Experimental results for different disordered polysaccharides, or for different concentrations of the same polysaccharide, converge to a single 'master curve' where η/η_0 is plotted as a function of $\dot{\gamma}/\dot{\gamma}_{1/2}$ (Morris, 1990). Departures from this general form of shear-thinning can therefore be regarded as diagnostic of structures other than disordered coils and/or of interactions other than physical entanglement.

Mechanical spectroscopy

Another route to detecting specific interactions in solution is by comparison of steady-shear viscosity, η, from 'large-deformation' measurements (e.g. in a rotational viscometer) with the corresponding 'dynamic viscosity', η^*, from small-deformation measurements using low-amplitude oscillation. For solutions of rigid, ordered species which associate to form a delicate 'weak gel' network (Clark & Ross-Murphy, 1987), the values obtained for η^* (characterising the unbroken network) are higher than those of η (where the network is broken down in making the measurement). However, when there are no such associations to break (as in solutions of entangled coils), η and η^* are closely superimposable (Cox & Merz, 1958) at equivalent values of shear rate ($\dot{\gamma}/s^{-1}$) and frequency of oscillation (ω/rad s^{-1}). Departures from Cox–Merz superposition are therefore indicative of enthalpic interactions in solution.

Oscillatory measurements also provide a powerful method for characterising liquid-like (viscous) and solid-like (elastic) response to imposed deformation (Ross-Murphy, 1984). The resistance of a solid is greatest at the extremes of the oscillatory cycle, where the deformation is greatest. The resistance of an idealised liquid, by contrast, is greatest at the midpoint of the cycle (where the net deformation is zero, but the *rate* of deformation is highest) and drops to zero at the extremes (where the rate of movement is zero). Solid and liquid response can therefore be characterised independently by resolving the overall resistance into components respectively 'in-phase' and 'out-of-phase' with the imposed deformation, and quantified as the 'storage' and 'loss' moduli (G' and G''). The tangent of the phase-lag (δ) between deformation and resistance provides a convenient index of the proportion of liquid-like character:

$$\tan \delta = G''/G' \tag{3}$$

EXPERIMENTAL

Methocel solutions were prepared by the following method. Approximately one-third of the total volume of

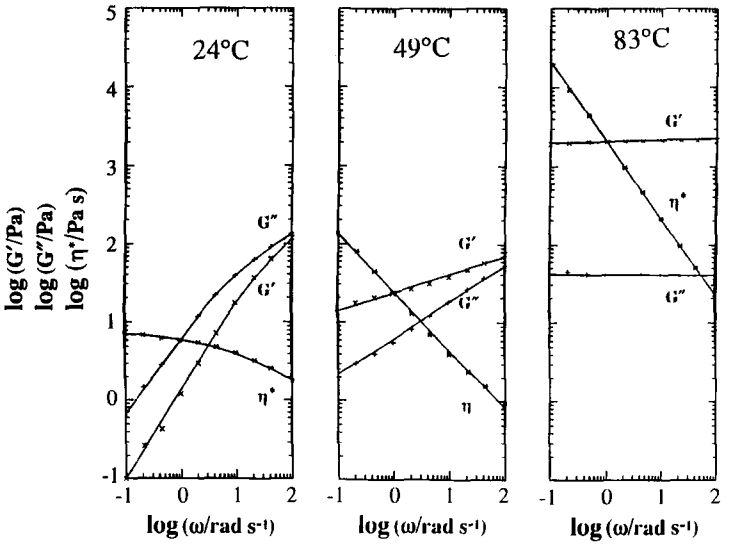

Fig. 1. Mechanical spectra (1% strain) for 2% (w/v) A4M at 24, 49 and 83°C, showing the variation of G' (×), G'' (+) and η^* (*) with frequency (ω).

water needed was heated to almost boiling (~95°C), and the polysaccharide was dispersed in it, by vigorous manual stirring, to give a thick, homogeneous paste. The remainder of the water was then added at ambient temperature, and stirring was continued until a clear solution was obtained (typically 30 min). The sample was then heated again to ~95°C, shaken vigorously to disrupt the gel, and degassed under reduced pressure in a vacuum desiccator. The heating, shaking, and evacuation steps were repeated until no further bubbles of gas were released under suction.

Rheological measurements under low-amplitude oscillatory shear were made using cone-and-plate geometry (50 mm radius; 0·02 rad cone angle) on a sensitive prototype rheometer designed and constructed in this Department by Dr R.K. Richardson. Temperature was controlled using a programmable circulating water bath and monitored by a thermocouple attached to the stationary element. The exposed periphery of the sample was coated with light silicone oil to minimise loss of water at high temperature. Steady-shear viscosity was measured on a Sangamo Viscoelastic Analyser, using a 50 mm, 2 degree cone-and-plate configuration.

DSC measurements were made using a Setaram microcalorimeter. Sample and reference pans were balanced to within 0·5 mg. Optical rotation was measured at 365 nm on a Perkin-Elmer 241 polarimeter, using a jacketed cell of pathlength 10 cm. Temperature was controlled by a circulating water bath and measured using a thermocouple in the neck of the cell (but out of the light path). Readings were taken after thermal equilibration at each temperature (typically 5 min). Measurements of light transmission were made at 460 nm and 1 cm pathlength using a Unicam SP 1800 spectrophotometer. ^{1}H-NMR spectra were recorded at 200 MHz on a Bruker AM200 spectrometer, using solutions prepared in D_2O rather than in water.

SOLUTION AND GEL RHEOLOGY

Figure 1 shows mechanical spectra (variation of G', G'' and η^* with frequency, ω) for 2% (w/v) A4M in the solution state at low temperature (24°C), in the gel state at high temperature (83°C), and at an intermediate temperature (49°C). The spectrum at low temperature is broadly similar to those of normal solutions of entangled polysaccharide coils (see, for example, Morris, 1984), with $G'' > G'$, both moduli increasing steeply with increasing ω, and η^* levelling off towards a 'Newtonian plateau' at low frequency. The high-temperature spectrum is typical of a strong gel network, with $G' \gg G''$, neither modulus showing any significant frequency dependence, and log η^* versus log ω descending steeply with a slope close to -1. At intermediate temperature (49°C) there is again evidence of some gel-like character ($G' > G''$), but with greater frequency dependence (particularly in G'') and less difference between the two moduli. The reason for choosing 49°C as a temperature for specific study will be explained later, in discussion of the temperature course of gelation.

Figure 2 shows the rheological changes observed when a sample (2% (w/v) A4M) was heated to 65°C and held there for $4\frac{1}{2}$ h. Over this period there was an approximately two-fold increase in both G' and G'' (with little variation in tan δ). Although not negligible, the development in moduli is small in comparison with the order-of-magnitude changes shown in Fig. 1, demonstrating that the gelation process is predominantly temperature dependent rather than time dependent.

As shown in Fig. 3(a), log G' for the high-temperature gel state has an approximately linear dependence on log c (for concentrations of A4M in the range $c = 0{\cdot}5$ to 2·5%, (w/v)), with a slope of 2·0 (i.e. G' is proportional to c^2). A c^2 dependence of gel strength is antici-

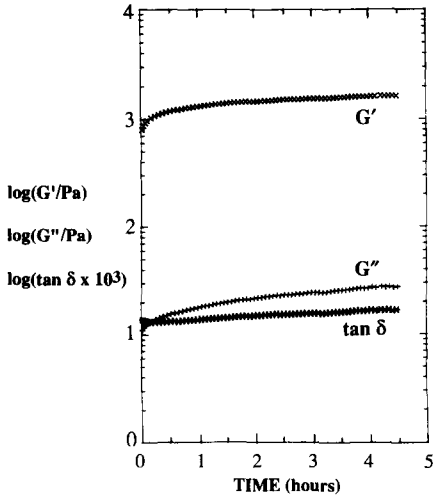

Fig. 2. Time dependence of G', G'' and tan δ (10 rad s^{-1}; 1% strain) for 2% (w/v) A4M at 65°C after heating from ambient temperature at 1 deg min^{-1}.

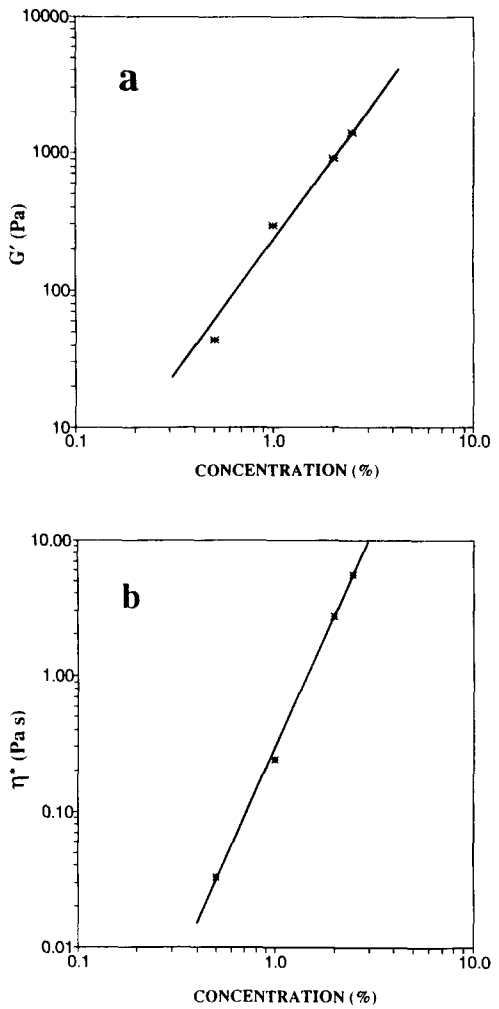

Fig. 3. (a) Concentration dependence of G' (10 rad s^{-1}; 1% strain) for A4M in the gel state at 72°C. (b) Concentration dependence of η^* (10 rad s^{-1}; 1% strain) for A4M in the solution state at 25°C.

pated theoretically (Clark & Ross-Murphy, 1987) for biopolymer gels at concentrations well above the minimum critical gelling concentration (c_0), if each chain can form a large number of intermolecular associations, and many natural biopolymers comply closely with this expectation (e.g. Smidsrød *et al.*, 1972; Ledward, 1986). The behaviour of the networks formed by 'hydrophobic' gelation of methylcellulose is therefore closely similar to that generated by enthalpic association of underivitised polysaccharides into co-operative junction zones.

Log η^* for the solution state at low temperature also shows a linear variation with log c (Fig. 3(b)). The slope of the double-logarithmic plot is ~3·3, the same as that observed (Morris *et al.*, 1981) for entangled polysaccharide coils. The comparison is not exact, since the generalisation of a $c^{3\cdot3}$ dependence of solution viscosity (at $c > c^*$) relates to 'zero-shear' viscosity (η_0) in the Newtonian plateau region, whereas the values shown in Fig. 3(b) were recorded at fixed frequency ($\omega = 10$ rad s^{-1}), in a spectral region where there is significant shear thinning (Fig. 1). The close correspondence, however, argues for molecular interactions broadly similar to the topological entanglements of underivatised polysaccharide coils.

As illustrated in Fig. 4, the similarity extends to close Cox–Merz superposition of the frequency dependence of η^* and shear rate dependence of η for solutions of methylcellulose. However, although the form of shear thinning shown in Fig. 4 is superficially similar to the generalised curve obtained (Morris *et al.*, 1981) for normal hydrophilic polysaccharides, quantitative analysis reveals an appreciable divergence of behaviour. Experimental 'flow curves' for entangled polysaccharide coils can be matched with good precision (Morris, 1990) by the equation:

$$\eta = \eta_0/[1 + (\dot{\gamma}/\dot{\gamma}_{1/2})^p] \quad (4)$$

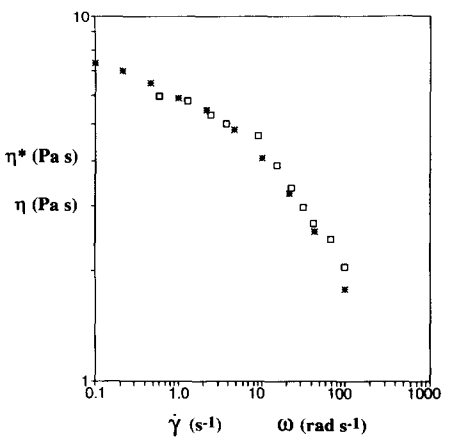

Fig. 4. Cox–Merz superposition of the shear-rate ($\dot{\gamma}$) dependence of η (□) and frequency (ω) dependence of η^* (*) for 2% (w/v) A4M in the solution state at 25°C.

which can be recast in the form of a linear relationship between η and $\eta\dot{\gamma}^p$:

$$\eta = \eta_0 - [(1/\dot{\gamma}_{1/2})^p]\eta\dot{\gamma}^p \quad (5)$$

It has been found empirically (Morris, 1984) that the exponent defining the curvature and terminal slope of log η versus log $\dot{\gamma}$ has the same value ($p = 0{\cdot}76$) for all disordered polysaccharides studied so far, yielding linear plots of η versus $\eta\dot{\gamma}^{0.76}$. As demonstrated in Fig. 5(a), however, the shear thinning of A4M (Fig. 4) shows obvious curvature when plotted in the same way.

The deviation from 'normal' polysaccharide behaviour was quantified using a simple computer program to vary the parameters η_0, $\dot{\gamma}_{1/2}$ and p in eqn (4) until the root-mean-square difference between observed and fitted values of η was minimised. The best fit to the data shown in Fig. 4 was obtained with $p = 0{\cdot}56$. Substituting this value in eqn (5) then gives a good linear plot for η versus $\eta\dot{\gamma}^p$ (Fig. 5(b)). Thus, although the solution properties of A4M resemble those of disordered hydrophilic polysaccharides, there is a significant difference in their response to changes in shear-rate and frequency, consistent with appreciable departure from 'random coil' geometry.

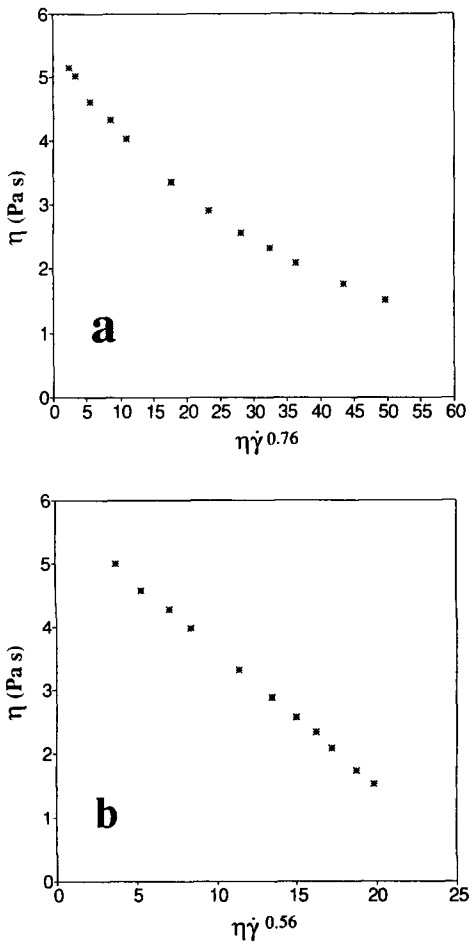

Fig. 5. Shear-rate dependence of viscosity for 2% (w/v) A4M (Fig. 4) plotted (eqn (4)) as η versus $\eta\dot{\gamma}^p$ · (a) $p = 0{\cdot}76$ (as for normal disordered polysaccharides); (b) $p = 0{\cdot}56$.

TEMPERATURE-COURSE OF RHEOLOGICAL CHANGES

Previous studies using steady-shear viscosity to monitor the thermogelation of methylcellulose (Sarkar, 1979) have shown an initial decrease in viscosity on heating, as commonly observed for other polymers, followed, at higher temperature, by a sharp increase associated with the onset of 'hydrophobic' gelation. A disadvantage of this approach, however, is that 'large-deformation' viscosity measurements may disrupt delicate networks as they form. In the present work we have therefore followed the temperature dependent changes in rheology using non-destructive oscillatory measurements.

Figure 6 shows the changes in rigidity (G') observed on heating and cooling a solution of A4M (1% (w/v)). In the initial stages of heating there is a reduction in G', mirroring the observed reduction in viscosity (Sarkar, 1979). Structure formation at higher temperature, however, occurs in two distinct 'waves', with two corresponding processes, offset to lower temperature, in dissociation of the gel network on cooling. The involvement of two separate processes is also evident (Fig. 7(a)) in the temperature dependence of tan δ (G''/G'), which gives an index of the proportion of liquid-like response.

The changes in G'' on heating (Fig. 7(b)) again show an initial decrease, with G'' then remaining virtually constant over the temperature range of the first increase in G', and rising steeply over the range of the second 'wave' of structure formation. In the cooling direction, the most noticeable feature is a transient increase in G'',

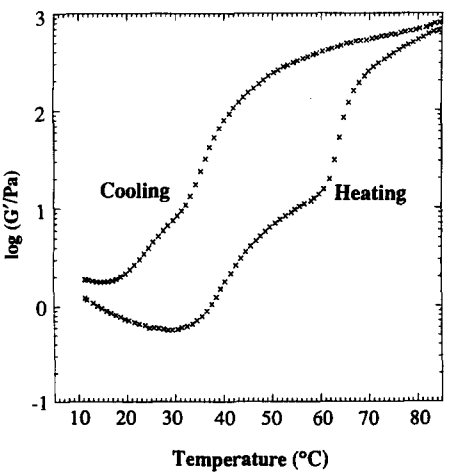

Fig. 6. Temperature dependence of G' (10 rad s^{-1}; 1% strain) for 1% (w/v) A4M on heating and cooling at 1 deg min^{-1}.

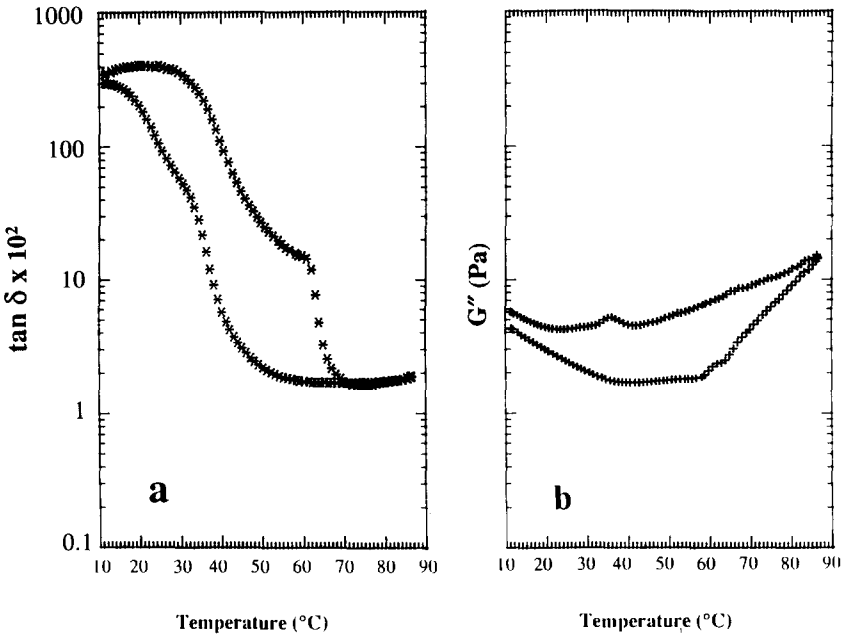

Fig. 7. Temperature dependence of (a) tan δ and (b) G'' for 1% (w/v) A4M. Conditions as in Fig. 6.

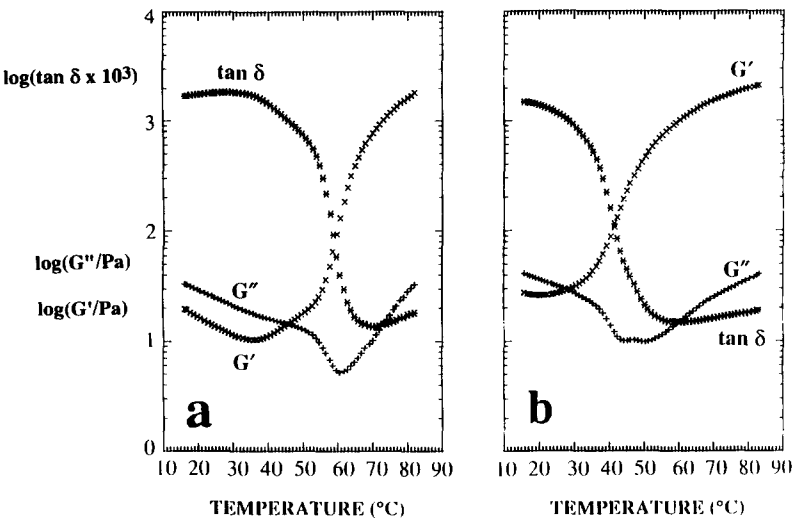

Fig. 8. Temperature dependence of G' (×), G'' (+) and tan δ (*) for 2% (w/v) A4M on (a) heating and (b) cooling. Conditions as in Fig. 6.

similar to the 'loss peaks' that are often observed in the final stages of melting of conventional gel networks (where they arise from release of large clusters of chains that are still linked together through residual junction zones).

Figure 8 shows the changes in G', G'' and tan δ on heating and cooling for a 2% (w/v) solution of A4M. At this higher concentration the first increase in G' is far less evident, and is accompanied by a significant reduction in G''. The changes observed in the cooling direction are also appreciably different in form from the corresponding changes at 1% (w/v), although they occur over essentially the same ranges of temperature. However, as shown in Fig. 1, the frequency dependence of the moduli changes drastically between low and high temperature, so that the precise form of the temperature dependent changes in rheological response will depend on the frequency at which the measurements were made.

Since the overall resistance to oscillatory deformation decreases with decreasing frequency (at fixed amplitude), there is a corresponding loss of precision and reliability in the moduli obtained. Most of the heating and cooling scans were therefore carried out at comparatively high frequency ($\omega = 10$ rad s^{-1}). Ideally, however, the frequency should be as low as possible, to minimise the contribution of entanglement coupling to solid-like response. This is illustrated in Fig. 9, which shows the development in rigidity on heating a 2% (w/v)

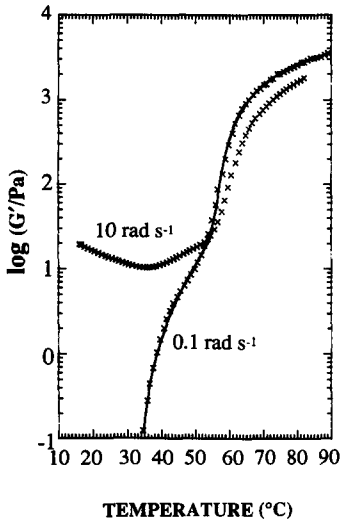

Fig. 9. Thermogelation of 2% (w/v) A4M, monitored by measurements of G' (1% strain) at 0·1 rad s^{-1} (solid line) and at 10 rad s^{-1} (symbols only).

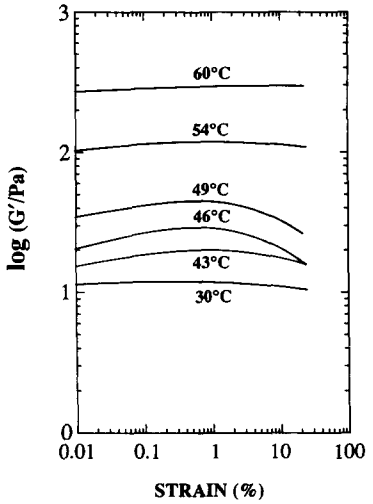

Fig. 10. Strain dependence of G' (10 rad s^{-1}) for 2% (w/v) A4M at 30, 43, 46, 49, 54 and 60°C.

solution of A4M, monitored by measurements of G' at 10 rad s^{-1} (as in Fig. 8(a)) and at 0·1 rad s^{-1}. The first increase in G', which at 10 rad s^{-1} is very small, becomes clearly evident at the lower frequency.

Figure 10 shows the strain dependence of G' for the same sample (2% (w/v) A4M) at various stages of the thermogelation process. In the solution state at low temperature, the modulus remains essentially constant up to the highest accessible amplitude of oscillation (~25% strain). There is then a progressive increase in strain dependence over the temperature range of the first 'wave' of structure-formation, but on moving into the range of the second process the modulus once more becomes independent of amplitude. The linear response at low and high temperature is consistent with the normal behaviour of, respectively, solutions and gels at moderate strain. The much greater strain dependence at intermediate temperature, towards completion of the first increase in G', indicates a delicate, easily disrupted network at this stage of structure-formation. The frequency dependence of mechanical response in the region of maximum strain dependence is illustrated in Fig. 1 by the spectrum recorded at 49°C. The overall response is gel-like ($G' > G''$), but with the moduli converging at higher frequency, as observed for solutions of entangled coils.

Figure 11 shows the temperature dependent changes in G' and G'' on heating and cooling for solutions of A4M at concentrations ranging from 0·25 to 2·5% (w/v). All measurements were made at 10 rad s^{-1} and 1% strain (which is within the linear region throughout the experimental temperature range; Fig. 10), using a fixed heating/cooling rate of 1 deg min^{-1}. Each family of curves shows a systematic progression of behaviour but, for the reasons discussed above, specific features of the thermal profiles are more evident at some concentrations than at others.

In particular, the first increase in G' on heating is accompanied, at the lower concentrations, by a steady increase in G''. With increasing concentration, however, as entanglement coupling in the solution state becomes progressively more significant, this increase in G'' is lost, and ultimately replaced by a sharp decrease. Similarly, the 'loss peak' that is evident in the otherwise featureless temperature dependence of G'' on cooling for 1% (w/v) A4M is obscured at higher or lower concentrations by the subsequent increase or decrease in modulus at lower temperature.

The initial decrease in G' in the early stages of heating is also particularly evident at 1%. At higher concentrations it is again obscured by the increasing contribution of entanglement coupling in solution, and at lower concentration it falls below the working range of the rheometer. The main conclusion to be drawn from Fig. 11, however, is that the rheological changes occur over essentially the same temperature-ranges at all concentrations studied. This is entirely consistent with results from the DSC investigations reported below.

DIFFERENTIAL SCANNING CALORIMETRY

Figure 11 includes illustrative DSC traces for 2% (w/v) A4M on heating and cooling at a scan rate of 0·1 deg min^{-1} (where thermal lag is negligible). In the heating direction there is a single endotherm which begins towards the end of the first 'wave' of increase in G' and continues through most of the second 'wave'. The cooling peak shows clear evidence of two separate processes, roughly coincident in temperature with the two 'waves' of reduction in G'.

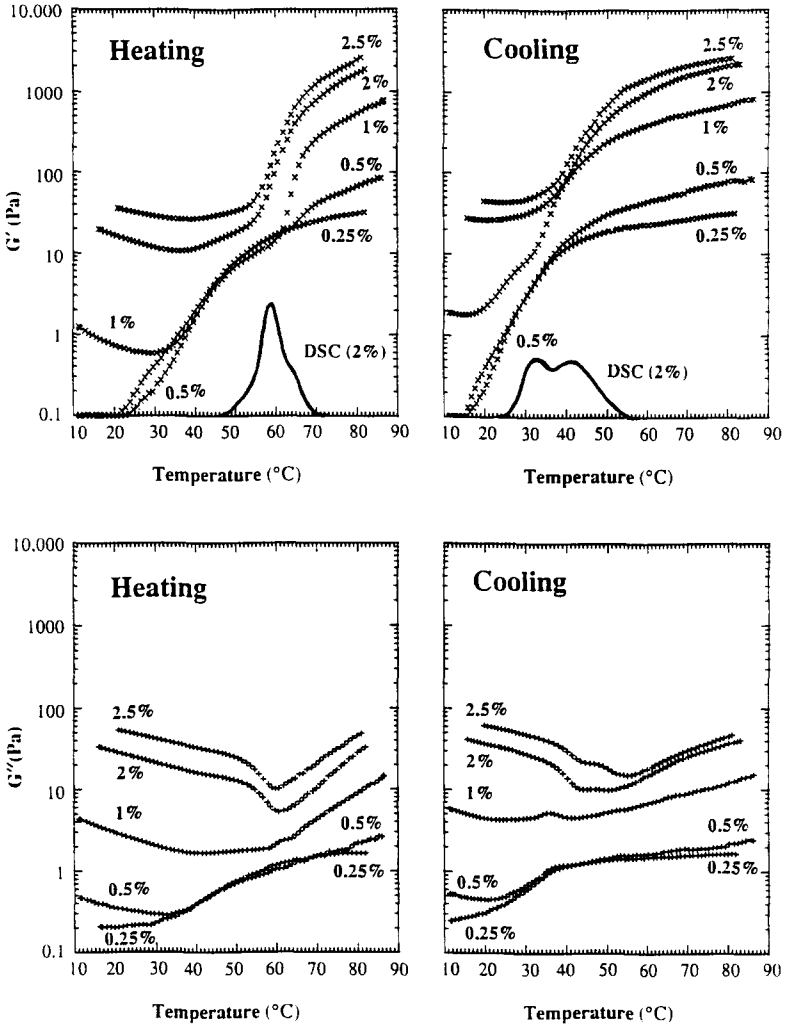

Fig. 11. Temperature dependence of G' and G'' (10 rad s^{-1}; 1% strain) for A4M at 0·25, 0·5, 1·0, 2·0 and 2·5% (w/v) on heating and cooling at 1 deg min^{-1}. The temperature course of thermal change in DSC (2%(w/v) A4M; 0·1 deg min^{-1}) is shown for direct comparison.

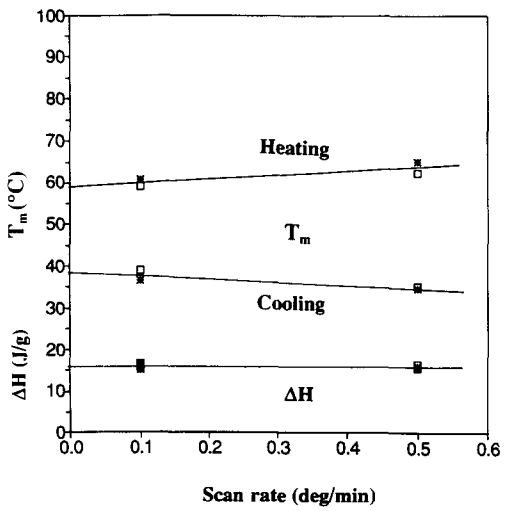

Fig. 12. Transition-midpoint temperatures (T_m) and enthalpy changes (ΔH) for 0·5% (*) and 2·0% (□) A4M from DSC scans at 0·1 and 0·5 deg min^{-1}.

As indicated in Fig. 12, the transition-midpoint temperatures show no significant concentration dependence, and extrapolate, at zero scan-rate, to $T_m \approx 59°C$ on heating and to $T_m \approx 38°C$ on cooling. The transition enthalpy is also independent of concentration (and scan-rate), and has a value of $\Delta H = 16 \pm 1$ J g^{-1}.

NUCLEAR MAGNETIC RESONANCE

Figure 13 shows illustrative ^{1}H-NMR spectra for A4M (1%(w/v) in D_2O) at various stages of the thermogelation process (at 30, 50 and 60°C). As in other polysaccharide systems, formation of the gel network is accompanied by a large reduction in discernible NMR signal. The large resonance at $\delta \approx 4.5$ ppm, which goes off-scale in the spectra shown, comes predominantly from HOD. The anomeric hydrogen atoms (at C-1 of the sugar rings) give resonances in the same spectral

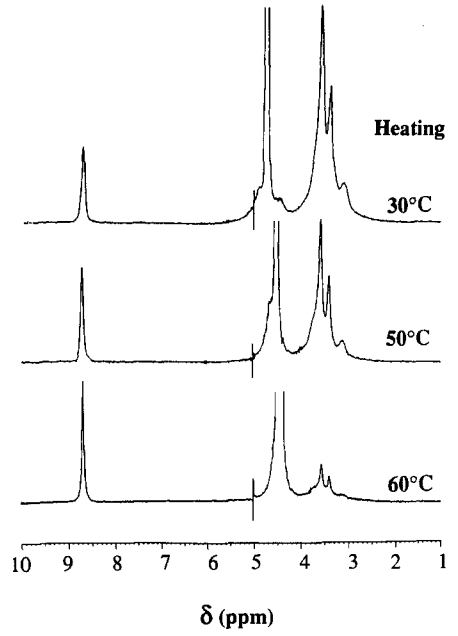

Fig. 13. ^{1}H-NMR spectra obtained for A4M (1%(w/v) in D_2O) on heating from ambient temperature. The signal at $\delta \approx 8{\cdot}7$ ppm is from the pyrazine standard used for comparison of integrated peak areas.

region, and are therefore obscured by the HOD peak. The resonances below $\delta \approx 4{\cdot}2$ ppm come from the other non-exchangeable protons of the cellulose chain, and from the methyl substituents.

The A4M sample used in the present work has DS = 1·81 (Dr N. Sarkar, pers. comm. 1992), corresponding to 5·43 methyl protons per sugar ring. The sugar itself has a further six non-exchangeable protons, two in the hydroxymethyl group at C-6 and one at each of C-2, C-3, C-4 and C-5. Thus, for a solution of fully disordered A4M, the integrated intensity of the NMR signal below 4·2 ppm should correspond to 11·43 protons per glucose ring.

The proportion of this anticipated maximum signal visible at each temperature was quantified by comparison with the integral obtained over the same spectral region for a known concentration of dextran, which remains conformationally disordered (and hence fully visible by NMR) at all temperatures, and which, like cellulose, has six non-exchangeable, non-anomeric protons per sugar ring. Relative spectral intensities were compared using a reference liquid (pyrazine) contained in a narrow capillary located within the NMR tube. In the spectra shown in Fig. 13, the pyrazine signal appears at $\delta \approx 8{\cdot}7$ ppm, well resolved from the polysaccharide resonances.

Figure 14 shows the changes in the proportion of visible NMR signal for A4M (1% (w/v)) during heat-induced gelation and subsequent dissociation of the gel on cooling. As observed rheologically (Fig. 6) and by DSC (Fig. 12), there is appreciable hysteresis between values recorded on heating and on cooling. The overall trend is towards higher intensity at lower temperatures, but there is a slight reduction in visible NMR with decreasing temperature at the bottom end of the range studied. At high temperature, the detectable signal is almost entirely suppressed, which is an expected consequence of the restricted mobility of polymer chains within a heavily crosslinked network. The maximum intensity in the sol state, however, is only ~60% of that anticipated for the fully visible signal, indicating that a substantial proportion of the polymer remains conformationally immobile in solution.

OPTICAL ROTATION AND TURBIDITY

Figure 15 shows the changes in optical rotation and light transmission observed on heating and cooling a solution of A4M. There is an initial increase in trans-

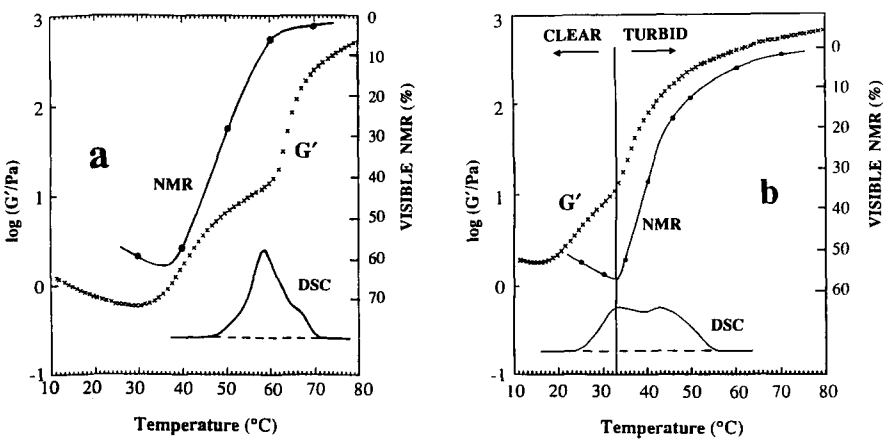

Fig. 14. Direct comparison of the temperature course of thermal, rheological and NMR changes for A4M on (a) heating and (b) cooling.

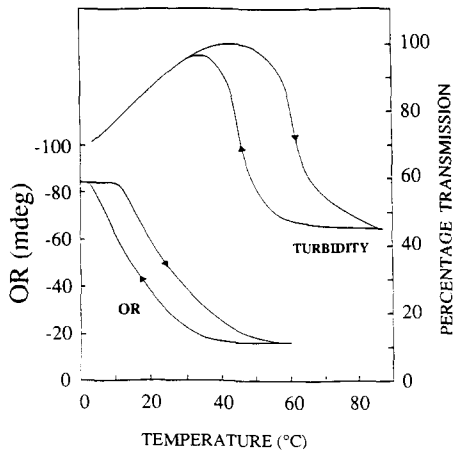

Fig. 15. Changes in conformation and turbidity of methylcellulose (0·25% (w/v) A4M) on heating and cooling, as monitored by, respectively, optical-rotation (10 cm pathlength; 365 nm) and percentage transmission (1 cm pathlength; 460 nm).

mission (i.e. decrease in turbidity) with increasing temperature, followed by a sharp increase in turbidity over the temperature range of the gelation process, with recovery of transmission then occurring at substantially lower temperature on cooling. The optical-rotation changes also show appreciable hysteresis, but are centred at much lower temperature.

PROPOSED INTERPRETATION

Solutions of methylcellulose (A4M) show an initial decrease in rigidity (G') on heating, followed by two distinct 'waves' of structure-formation, with two corresponding processes (offset to lower temperature) on cooling. Both are accompanied (Fig. 14) by enthalpy changes in DSC. The transition from one process to the other corresponds to the maximum in detectable high-resolution ^{1}H-NMR signal (i.e. to maximum mobility of the polysaccharide chains). Transmission of light through the sample (Fig. 15) also reaches a maximum value at this point, with substantial reduction at both higher and lower temperature. Optical rotation measurements (Fig. 15) show clear evidence of a conformational transition accompanying the changes in transmission over the lower temperature range.

The obvious interpretation of this behaviour is that there are structures present in solutions of methylcellulose at low temperature which melt out during the initial stages of heating and, in doing so, allow the development of a different structure at higher temperature. A direct analogy would be the thermal gelation of globular proteins (Tanford, 1980; Clark & Ross-Murphy, 1987), where unfolding of the native globule is a necessary precursor to network formation by intermolecular association of exposed hydrophobic regions from the protein core.

The absolute intensity of visible ^{1}H-NMR (Fig. 14) gives direct evidence of conformational rigidity in solution, since a significant proportion of the signal remains undetectable at low temperature. The anomalous shear thinning behaviour of Methocel solutions (Fig. 5) also argues for a departure from 'random coil' geometry, although the concentration dependence of viscosity (Fig. 3(b)) and Cox–Merz superposition of η and η^* (Fig. 4) are consistent with topological entanglement rather than any enthalpic interactions between individual species.

The results of the present investigation give no direct indication of the nature of the ordered structure in solution. A likely possibility, however, is that during chemical derivitisation small regions of native cellulose structure remain intact, linking several chains together into bundles, with long regions of heavy substitution interspersed by shorter stretches of low (or zero) substitution along each bundle. The methyl groups in regions of dense substitution would then have natural partners for hydrophobic clustering, again directly analogous to the interior of globular proteins.

Partial dissociation of these clusters in the early stages of heating (Fig. 16) would explain the increase in detectable NMR (Fig. 14), the decrease in turbidity (Fig. 15), the reduction in G' (Fig. 14) and the onset of the conformational change detected by optical rotation (Fig. 15). The first increase in G', accompanied by continuation of the change in optical rotation, may then be interpreted as arising from separation of the constituent strands at the ends of the bundles, with consequent massive increase in hydrodynamic volume, analogous to the swelling of starch granules into a viscoelastic paste on gelatinisation. In partial support of this interpretation, the mechanical spectra obtained towards the end of the first process (at 49°C; Fig. 1) show a significant frequency dependence of both moduli, and reduction in G' with increasing amplitude of oscillation (showing structural breakdown) begins (Fig. 10) at far lower strain than in normal gels, consistent with weak, topological interactions between the swollen bundles.

Exposure of hydrophobic (methyl) substituents to the aqueous environment during swelling of the postulated 'bundles' would be expected to lead to formation of the structured water 'cages' discussed above. The second increase in G' (Fig. 14) can then be attributed to thermal disruption of the cage structures, with consequent formation of the final, strong, gel network by hydrophobic association of strands radiating from different bundles (Fig. 16). Involvement of residual cellulosic structure in network crosslinking would offer a direct explanation of why methylcelluloses prepared under homogenous conditions (with, therefore, a more even distribution of substituents) do not gel (Takahashi *et al.*, 1987).

Although still highly speculative, the proposed model is consistent with the established properties of other

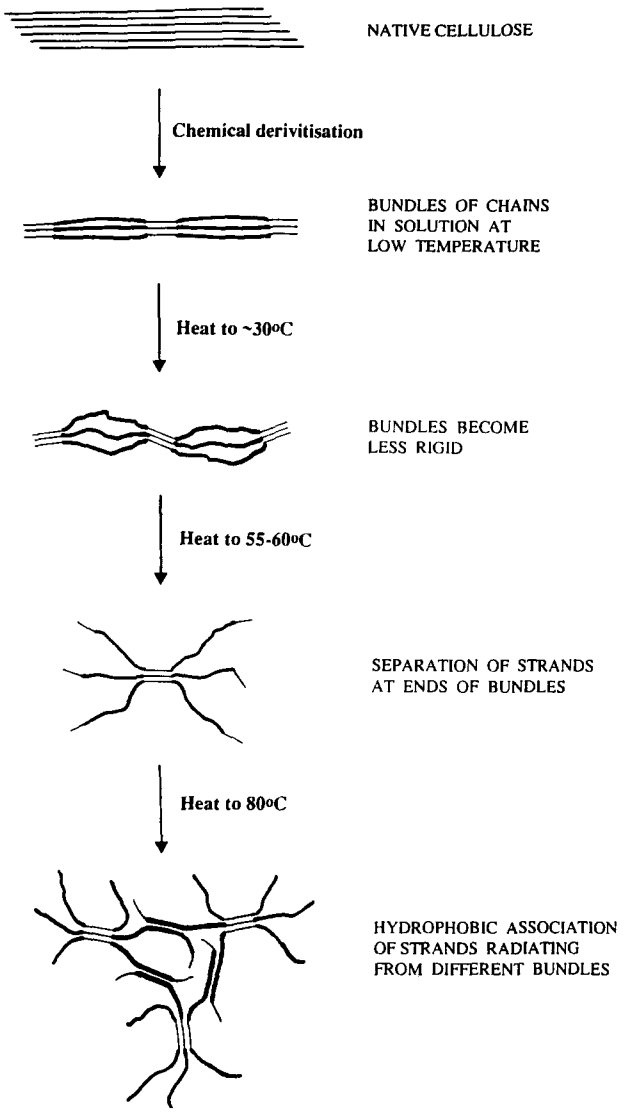

Fig. 16. Schematic illustration of the postulated structures and processes involved in the thermogelation of Methocel. Faint lines denote unsubstituted or sparingly substituted chain segments; bold lines denote regions of dense substitution.

gelling biopolymers. In particular, the thermal hysteresis in optical rotation (Fig. 15) is closely similar to that observed for underivitised polysaccharides such as agarose and kappa-carrageenan (Rees *et al.*, 1982), where conformational ordering on cooling is accompanied by aggregation of the ordered structures, with melting of the aggregates then occurring over a higher temperature range. Dissociation of the cellulosic 'bundles' would similarly be expected to occur at higher temperatures than those at which the bundles will form again on cooling.

By extension of this argument, dissociation of the gel network on cooling may reflect the relative stabilities of molecular association within and between the bundles. Adoption of the proposed fibrillar structure might be expected to maximise favourable enthalpic interactions, but cause a severe loss of entropy. Conversely, the entropy of a gel network structure would be higher, but the degree of ordered packing would be decreased. Conversion from the fibrillar structure at low temperature to the network structure at high temperature, with the converse change on cooling, would then be an expected consequence of the increasing importance of entropy with increasing temperature (as in the formation and melting of other polysaccharide gels).

In terms of the proposed model (Fig. 16) the single endotherm observed on heating solutions of A4M (Fig. 14(a)) would include contributions from both the heat required to dissociate a proportion of the residual cellulosic stretches within the 'bundles' (allowing strands to separate) and the heat required to 'melt' the water cages formed around methyl substituents exposed in the earlier stages of swelling. The two processes contributing to the bimodal exotherm observed on cooling may be tentatively assigned to, respectively, formation of water cages around the methyl groups re-exposed to the aqueous environment during dissociation of the gel network, and re-establishment of the postulated 'bundles' at lower temperature.

The proposal that dissociation of methylcellulose gels is driven by reversion to a more thermodynamically stable 'bundle' structure is supported by studies of the effect of an amphiphilic cosolute (Haque *et al.*, 1994). Addition of increasing concentrations of ethylene glycol was found to have little effect on the second, major, process in thermogelation of A4M, but caused a progressive increase in G' for the solution state towards the value attained in water after completion of the first 'wave' of structure-formation (cf. Fig. 6). In terms of the model outlined in Fig. 16, this behaviour suggests increasing solubilisation of the cellulosic bundles. By 40% (v/v) ethylene glycol the modulus remained virtually independent of temperature up to the onset of the second structuring process, indicating complete dissociation of cellulosic structure. Significantly, the resulting gels then remained intact on cooling to 0°C, as expected from the interpretation proposed here.

ACKNOWLEDGEMENTS

We thank Dr M.J. Gidley and Mr D.C. Caswell (Unilever Research) for NMR measurements; Dr N. Sarkar and Dr P. Smith (Dow Chemical Company) for helpful discussions; and The British Council for the award of a Study Fellowship to one of us (A.H.).

REFERENCES

Cantor, C.R. & Schimmel, P.R. (1980). *Biophysical Chemistry*. Freeman, New York.

Clark, A.H. & Ross-Murphy, S.B. (1987). *Advan. Polym. Sci.*, **83**, 57–192.

Cox, W.P. & Merz, E.H. (1958). *J. Polym. Sci.*, **28,** 619–22.
Franks, F. (1983). *Water.* Royal Society of Chemistry, London.
Graessley, W.W. (1974). *Advan. Polym. Sci.*, **16,** 1–179.
Greminger, G.K., Jr & Savage, A.B. (1973). In *Industrial Gums,* eds R.L. Whistler & J.N. BeMiller. Academic Press, New York, pp. 619–47.
Grover, J.A. (1986). In *Food Hydrocolloids, Vol. 3,* ed. M. Glicksman. CRC Press, Boca Raton, FL, pp. 121–54.
Haque, A., Morris, E.R. & Richardson, R.K. (1993*a*). In *Frontiers in Carbohydrate Research 3,* eds T. Eads, R.P. Millane, J.N. BeMiller & R. Chandrasekaran. Elsevier, New York (in press).
Haque, A., Richardson, R.K., Morris, E.R., Gidley, M.J. & Caswell, D.C. (1993*b*). *Carbohydr. Polym.*, **22,** 175–86, (this issue).
Haque, A., Jones, A.K., Richardson, R.K. & Morris, E.R. (1994). In *Gums and Stabilisers for the Food Industry 7,* eds G.O. Phillips, P.A. Williams & D.J. Wedlock, IRL Press, Oxford, UK (in press).
Heymann, E. (1935). *Trans. Faraday Soc.*, **31,** 846–64.
Ledward, D.A. (1986). In *Functional Properties of Food Macromolecules,* eds J.R. Mitchell & D.A. Ledward. Elsevier, London, pp. 171–201.
Morris, E.R. (1984). In *Gums and Stabilisers for the Food Industry 2,* eds G.O. Philips, D.J. Wedlock & P.A. Williams. Pergamon Press, Oxford, UK, pp. 57–78.
Morris, E.R. (1990). *Carbohydr. Polym.*, **13,** 85–96.
Morris, E.R., Cutler, A.N., Ross-Murphy, S.B., Rees, D.A. & Price, J. (1981). *Carbohydr. Polym.*, **1,** 5–21.
Rees, D.A. (1969). *Advan. Carbohydr. Chem. Biochem.*, **24,** 267–332.
Rees, D.A., Morris, E.R., Thom, D. & Madden, J.K. (1982). In *The Polysaccharides, Vol. 1,* ed. G.O. Aspinall, Academic Press, New York, pp. 195–290.
Ross-Murphy, S.B. (1984). In *Biophysical Methods in Food Research,* ed. H.W.-S. Chan. Critical Reports on Applied Chemistry, SCI, London, pp. 138–99.
Sarkar, N. (1979). *J. Appl. Polym. Sci.*, **24,** 1073–87.
Smidsrød, O., Haug, A. & Lian, B. (1972). *Acta Chem. Scand.*, **26,** 71–8.
Takahashi, S.-I., Fujimoto, T., Miyamoto, T. & Inagaki, H. (1987). *J. Polym. Sci. A.*, **25,** 987–94.
Tanford, C. (1980). *The Hydrophobic Effect: Formation of Micelles and Biological Membranes.* John Wiley, New York.
Wright, D.J. (1984). In *Biophysical Methods in Food Research,* ed. H.W.-S. Chan. Critical Reports on Applied Chemistry, SCI, London, pp. 1–36.